Vol 447|3 May 2007|doi:10.1038/nature05687

ARTICLES

The structure of a plant photosystem I supercomplex at 3.4 Å resolution

Alexey Amunts[1], Omri Drory[1] & Nathan Nelson[1]

All higher organisms on Earth receive energy directly or indirectly from oxygenic photosynthesis performed by plants, green algae and cyanobacteria. Photosystem I (PSI) is a supercomplex of a reaction centre and light-harvesting complexes. It generates the most negative redox potential in nature, and thus largely determines the global amount of enthalpy in living systems. We report the structure of plant PSI at 3.4 Å resolution, revealing 17 protein subunits. PsaN was identified in the luminal side of the supercomplex, and most of the amino acids in the reaction centre were traced. The crystal structure of PSI provides a picture at near atomic detail of 11 out of 12 protein subunits of the reaction centre. At this level, 168 chlorophylls (65 assigned with orientations for Q_x and Q_y transition dipole moments), 2 phylloquinones, 3 Fe_4S_4 clusters and 5 carotenoids are described. This structural information extends the understanding of the most efficient nano-photochemical machine in nature.

Oxygenic photosynthesis is the principal producer of both oxygen and organic matter on Earth[1–3]. Water, the electron donor for this process, is oxidized to O_2 and four protons by PSII. The electrons that have been extracted from water are shuttled through a quinone pool and the cytochrome b_6f complex to plastocyanin—a small, soluble, copper-containing protein. Solar energy that has been absorbed by PSI induces the translocation of an electron from plastocyanin at the inner face of the membrane (thylakoid lumen) to ferredoxin on the opposite side (stroma). PSI generates the most negative redox potential in nature (−1 V), and thus largely determines the global amount of enthalpy in living systems. The structures of three of the four complexes that catalyse oxygenic photosynthesis in cyanobacteria have been solved at relatively high resolution, and the position of most of their amino acids and prosthetic groups has been defined[4–8]. Thus, the architecture of oxygenic photosynthesis in cyanobacteria has largely been determined. The structure of cytochrome b_6f complex from chloroplasts of the algae *Chlamydomonas reinhardtii* has also been solved at high resolution, and has remarkable similarity to the cyanobacterial complex[9]. Recently, two high-resolution structures of light-harvesting complexes of PSII from higher plants were published[10,11].

In a previous study, we crystallized and determined the structure of plant PSI at an intermediate resolution of 4.4 Å[12,13]. A model of α-carbon chains of 16 subunits, 45 transmembrane helices, 2 phylloquinones, 3 iron–sulphur clusters and 167 chlorophyll molecules was presented. To understand better the role of the protein subunits and individual amino acids in the binding and organization of the various cofactors, as well as the interaction between the cofactors, we have determined the X-ray crystallographic structure of PSI from pea (*Pisum sativum*) at 3.4 Å resolution, and we describe a near atomic model of the system.

Features revealed by the new structure

The new crystal form contains one complex in the asymmetric unit, with unit cell parameters $a = 124.87$ Å, $b = 187.27$ Å, $c = 131.96$ Å, $\beta = 91.03^\circ$ (Supplementary Information and Supplementary Fig. 1). In the electron density map, all the previously detected 16 subunits of PSI were identified, and PsaN was also detected (Fig. 1). Twelve of the subunits (PsaA, B, C, D, E, F, G, H, I, J, L, and N; ref. 14) were interpreted with the known amino acid sequences from pea and *Arabidopsis thaliana* plants (Supplementary Tables 1 and 2). The position of 3,038 out of 3,443 predicted amino acids was assigned; for 2,909 of them, side chains were built into the model. Part of PsaK could be modelled as polyalanine, because the electron density was not as well defined in this part of the supercomplex. Subunit O (ref. 15), which was identified in preparations of plant PSI, was not

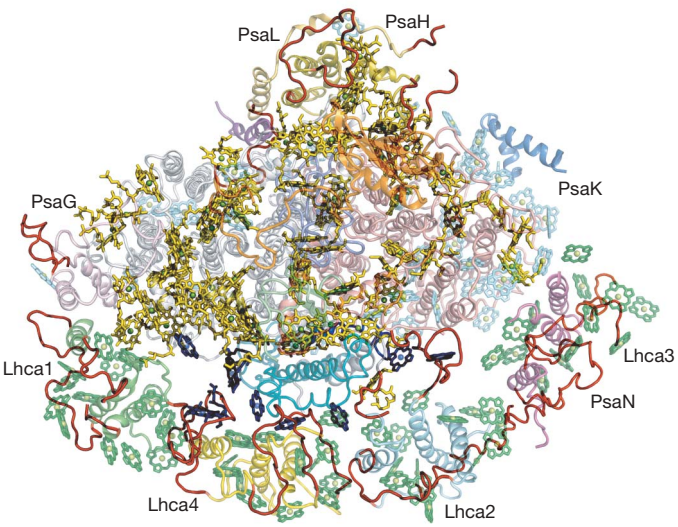

Figure 1 | The structural model of plant photosystem I at 3.4 Å resolution. View from the stroma of the structure of plant PSI. Novel structural elements that are not present in the previous model are shown as red ribbon structures. Chlorophylls with detected phytyl side chains, revealing the orientation of the Q_x and Q_y transition dipole moments, are yellow. The rest of the reaction centre chlorophylls are cyan, gap chlorophylls are blue and chlorophylls of LHCI are green. The positions of PsaG, H, K, L and N, as well as the various LHCI monomers, are indicated. Each individual subunit is coloured differently.

[1]Department of Biochemistry, The George S. Wise Faculty of Life Sciences, The Daniella Rich Institute for Structural Biology, Tel Aviv University, Tel Aviv, 69978, Israel.

present in the crystal and there was no space for it to be accommodated. Subunit P (ref. 16) could not be positively identified, but unassigned electron density close to PsaH could possibly be assigned to this subunit. PsaN, which was not detected in the 4.4 Å structure, was identified and its amino and carboxy termini were determined by partial amino acid tracing (Fig. 1). The entire length of PsaG was traced and the interaction of its loop with PsaB gives credence to the conclusions of a recent mutational analysis[17]. The positive amino acids that are present in the loop are protected from proteases by close proximity to the membrane (Lys 59), salt bridge formation (Arg 50 with Glu 306 of PsaB) and tight interaction with PsaB (Lys 52). A major part of Lhca1–4 was assigned using the corresponding amino acids, but parts of the loops that could be detected were modelled by amino acids without side chains. Tracing amino acids of the transmembrane helices of Lhca1–4 allowed positive identification of the four light-harvesting subunits. For the 168 chlorophylls, the position and Q_z orientation of the head groups were determined. For 65 of the chlorophylls, the ring substituents (and part of their phytyl side chains) could be modelled into the electron density map, revealing the orientation of the Q_x and Q_y transition dipole moments.

The PSI reaction centre complex

The two principal subunits of the reaction centre, PsaA and PsaB, share similarities in their amino acid sequences and constitute a pseudosymmetric structure that evolved from an ancient homodimeric assembly[3,18]. Together, the subunits harbour the electron transport chain (ETC), which is the heart of PSI and functions in the photoelectrochemical reaction of the system. In addition, two reaction centre proteins are exclusively present in plants and green algae (subunits G and H). The position and shape of PsaH conform well to its proposed role as a docking site for light harvesting complex (LHC)II (ref. 19). Part of the N terminus that was not detected in the previous report was traced in the current study (Fig. 1) and was found to form an additional surface that may be used for controlled binding of LHCII and other auxiliary factors. On the opposite side of the reaction centre, PsaG and its two tilting transmembrane helices contribute most of the contact surface area for association with LHCI (ref. 13). Twenty amino acids of the PsaG C terminus (Fig. 1) protrude out of the generally compact structure in this area; this may provide a binding surface for other membrane complexes such as the cytochrome b_6f complex. The electron densities at the centre were clear enough to correct potential sequencing mistakes (Supplementary Fig. 2). For example, there is an arginine residue in the sequence of pea chloroplasts at position 220 of PsaA; in all other plants, there is a glycine residue at the same position. The electron density obtained here leaves little doubt that, in PsaA from pea, there is also a glycine residue at this position. On the luminal side, the most noticeable distinction between plant and cyanobacterial reaction centres is the helix–loop–helix motif contributed by the longer N-terminal domain of plant PsaF (Fig. 2a and Supplementary Fig. 3). This domain enables more efficient plastocyanin binding in plants and, as a result, two orders of magnitude faster electron transfer from the copper protein to P700 (ref. 13). On the stromal side of PSI, where ferredoxin and ferredoxin-NADP-reductase bind, almost all amino acids of PsaC, PsaD and PsaE were traced. The hypothetical amino acid chain T was not visible in the current electron densities.

The PsaA/B part of the ETC is formed by six chlorophylls, two phylloquinones and one out of the three Fe_4S_4 clusters of PSI (Fig. 2a). The chlorophylls and quinones are arranged in two branches (A and B) as pairs of molecules related by a pseudo-C2 axis. The two chlorophylls that constitute the P700, and most other chlorophylls at the centre, seem to be identically positioned to those reported for the cyanobacterium *Synechococcus elongatus*[4]. The amino acids involved in Mg^{2+} coordination and hydrogen bonding to the second and third Chla pairs of the ETC are strictly conserved between the PsaA and PsaB, in species from cyanobacteria to higher plants[4]. One of the unsolved questions in the mechanism of the ETC is whether the Chla from one, or both (PsaA and PsaB), branches are active in electron transport[8]. Several electron paramagnetic resonance (EPR) experiments with cyanobacterial PSI suggest that most of the electron transfer is conducted by the A branch[20]; however, fast spectroscopic experiments with algae suggest an equal share of the two branches in electron transfer[21]. Even though small changes in the cofactor positions were detected, the current resolution does not permit a definite answer to this question.

Chlorophylls and carotenes at the reaction centre

The core complex (reaction centre) of plant PSI contains approximately 100 chlorophyll molecules, of which a vast majority maintain an almost identical position, as in cyanobacterial PSI[13]. For 65

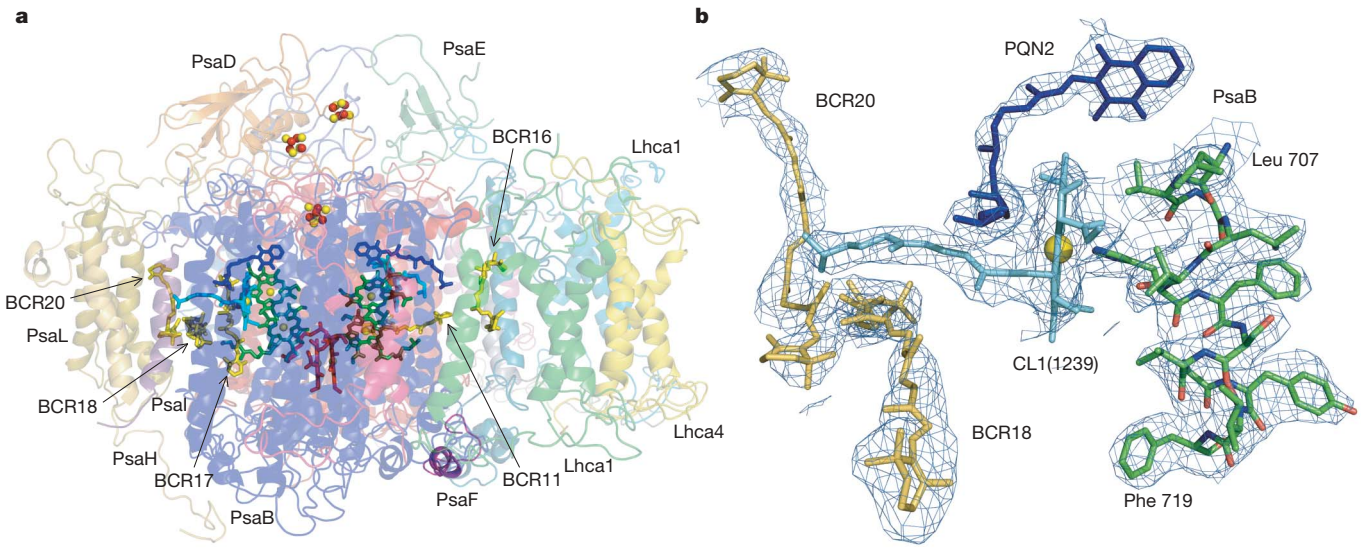

Figure 2 | Position of β-carotenes in relation to the ETC. a, The ETC, two additional chlorophylls and three β-carotene molecules are depicted on the background of the subunit structure of PSI. Red, P700 chlorophylls 9010 and 9011; green, ETC chlorophylls 9012, 9013, 9022 and 9023; cyan, chlorophylls 1239 and 1140; yellow, β-carotenes 6011and 6018; and blue, phylloquinones. The three sulphur–iron clusters are shown as spheres in red (iron) and yellow (sulphur). **b**, The $2F_oF_c$ electron density map (1σ), covering β-carotenes 6018 and 6020 (BCR18 and BCR20), chlorophyll 1239 (CL1(1239)), and phylloquinone 5002 (PQN2), as well as part of PsaB (amino acids 707–719). Colour codes correspond to Fig. 3a.

molecules, the electron densities were good enough to trace part of their phytyl side chains, revealing the Q_x and Q_y transition dipole moments (Fig. 1). These chlorophylls exhibit a remarkable conservation in their position and orientation compared to those of *S. elongatus*[4]. As expected, the chlorophylls that are coordinated to subunits M and X in cyanobacteria were missing in the plant reaction centre.

The construction of our model was aided by a theoretical atomic model of plant PSI that was built by combining the low-resolution model of plant PSI[13], the high resolution structure of the cyanobacteria PSI[4], and a new approach of molecular dynamics[22]. The position and orientation of most chlorophyll molecules of the current model are in accordance with the theoretical model. However, the refined position of several chlorophyll molecules was significantly different from the theoretical model. Plant PSI contains 19 chlorophyll molecules, including 9 gap chlorophylls (Fig. 1), that are not present in the cyanobacterial reaction centre and are not part of the LHCI monomers[23,24]. In the neighbourhood of PsaK, we modelled four chlorophyll molecules, some of which may have an important role in excitation energy transfer from LHCII to PSI (see below). This side of PSI is poorly resolved not only in the larger plant PSI but also in the high-resolution PSI of *S. elongatus*[4].

Over 20 carotene molecules are expected to be present in plant PSI (ref. 22). Relatively good electron densities allowed for the assignment of five β-carotene (BCR) molecules in various locations of the reaction centre (Fig. 2). BCR11 is situated in a strategic location in the vicinity of the proposed excitation energy transfer pathway from the reaction centre antenna to the ETC—approximately 10 Å away from P700—and one of its poles is 3 Å away from Chl1126 and thus adjacent to Trp 747/A and His 389/A. The second pole is 6 Å away from Chl1230, which is coordinated by His 439/B, and 4.5 Å from Chl1229, and is in the vicinity of Phe 90/F. This BCR is located at a similar position to β-carotene in the cyanobacterial PSI and in the proposed theoretical model of plant PSI[22]. However, BCR16 moved considerably from its position in *S. elongatus*[4]—because subunit X is not present in plant PSI, the chlorophyll molecule that it coordinated is missing and two gap chlorophyll molecules (Chl1302 and Chl1303) were added to the plant complex. One of the poles of BCR16 is as close as 3.3 Å to Chl1303, and the other pole is situated 5 and 4.3 Å from Trp 99/F and Trp 136/F, respectively. Most of the β-carotenes in cyanobacteria were located in pockets of hydrophobic residues that are highly conserved between cyanobacteria and plants. This arrangement may protect not only from triplets that are formed by the pigment molecules but also from destruction of aromatic amino acids by ultraviolet light. BCR17 is coordinated by Trp 648/B and Trp 646/B; Phe 652/B and Phe 719/B are situated in its vicinity (Fig. 2). BCR17, 18 and 20 are close to each other, suggesting potential radiation damage in this part of the reaction centre.

Light-harvesting complex I

The LHCI belt, with its associated chlorophylls, is the most prominent addition to PSI structure by plants and green algae. The LHCI belt contributes a mass of 160 kDa out of approximately 600 kDa in PSI. LHCI is composed of four nuclear gene products (Lhca1–Lhca4) that are 20–24 kDa polypeptides and belong to the LHC family of chlorophyll a/b binding proteins. The archetype of this family, and the most abundant membrane protein in nature, is the major LHCII protein (Lhcb1–2), the structure of which was recently elucidated by X-ray crystallography at 2.7 (ref. 10) and 2.5 Å (ref. 11) resolution. The identification of the four Lhca proteins in plant PSI was based on a large body of biochemical experiments[13,25–27]. We were able to positively identify the four LHCI units as Lhca1, Lhca4, Lhca2 and Lhca3, starting at the G-pole of the reaction centre, respectively. This was achieved by assigning electron densities to corresponding amino acids with large side chains that are unique to each LHCI protein. Binding of LHCI to the reaction centre is asymmetric, namely, much stronger on the G-pole than on the K-pole of the core (Fig. 1). The other LHCI proteins interact with the core mainly through small binding surfaces at their stromally exposed regions (Fig. 1). Lhca4 binds to PsaF, Lhca2 associates weakly with PsaJ, and Lhca3 binds weakly to PsaA.

Even though the light harvesting chlorophyll a/b binding proteins that constitute the peripheral antennas of PSI (LHCI) and PSII (LHCII) share sequence and structural homology, their oligomeric states vary considerably. Whereas LHCI proteins assemble into dimers, the light harvesting proteins that associate with PSII form either trimers (LHCII), or monomers as minor antenna members CP24, CP26 and CP29 (ref. 1). The current model permitted a closer look at the dimer formation and mode of interaction between the LHCI monomers and reaction centre subunits (Fig. 3a). Both Lhca1–4 and LHCII bind 14 chlorophyll a/b molecules each (Fig. 1), and possess the LHCII general fold[10,11,13,28]. The absorption peak of the 'bulk' chlorophylls of LHCI proteins is also shifted to lower energies compared with LHCII[13,24,29]. Dimerization in LHCI is mediated by relatively small contact surfaces at the luminal side by the C terminus and at the stromal side of the N-terminal domain of the Lhca

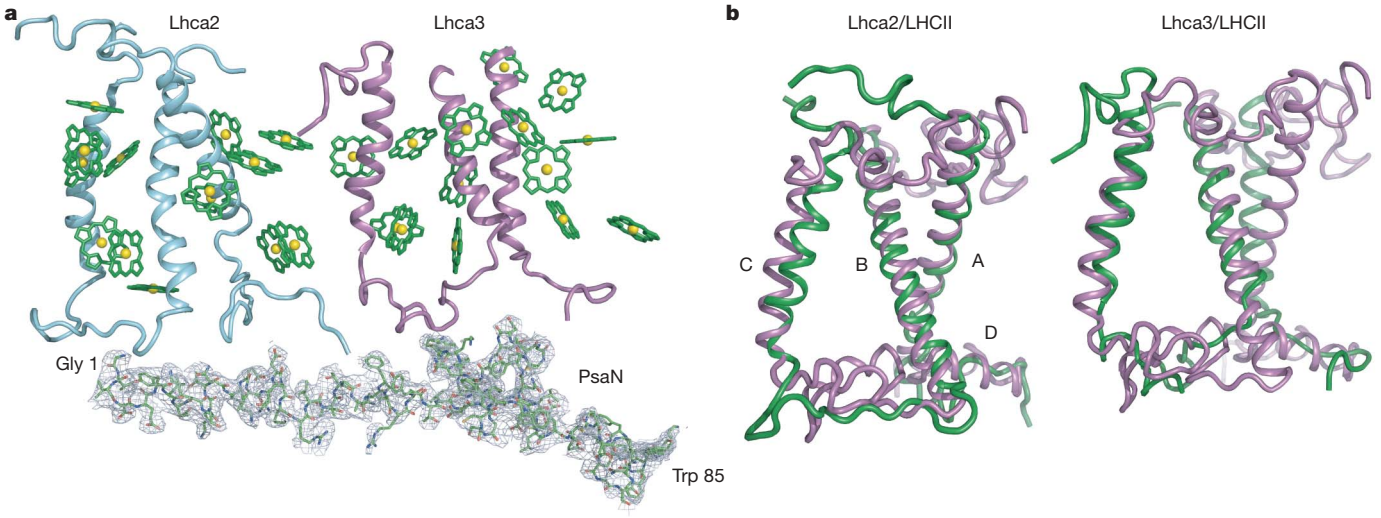

Figure 3 | The position of PsaN in relation to Lhca2 and Lhca3, and the unique fold of Lhca3. **a**, The $2F_oF_c$ (1σ) electron density map covering PsaN, and the structure of the Lhca2–Lhca3 heterodimer. Cyan, Lhca2; magenta, Lhca3; green, chlorophylls; yellow, magnesium atoms. **b**, Left panel, superposition of LHCII (magenta) on Lhca2 (green); right panel, superposition of LHCII (magenta) on Lhca3 (green).

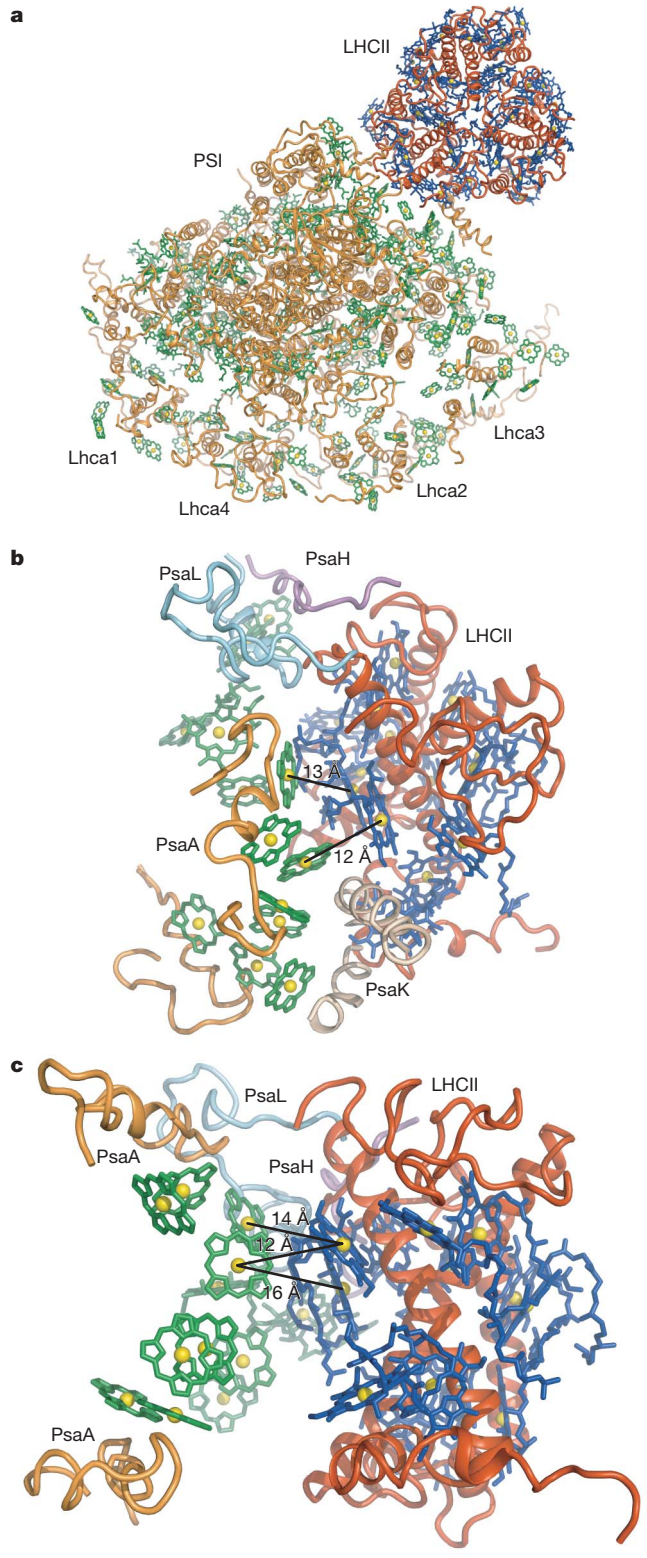

Figure 4 | Model for PSI–LHCII interactions. The structural models of plant PSI and the LHCII trimer were fitted by accommodating a possible binding site at the PsaK side. In this position, LHCII could be readily crosslinked to subunits PsaL and PsaH, but it is too far to crosslink with PsaI. The initial docking was made by modified PatchDock software (http://bioinfo3d.cs.tau.ac.il). The fit was manually improved to better agree with experimental data. **a**, A view from the stroma of plant PSI together with a LHCII trimer (Protein Data Bank code, 2BHW; ref. 11). The PSI complex (orange), PSI chlorophylls (green), LHCII trimer (red), LHCII chlorophylls (blue) and chlorophyll magnesium atoms (yellow) are shown. **b**, **c**, An enlarged view from the stroma (**b**) and a view along the membrane plane (**b**), of the suggested PSI–LHCII interaction site. LHCII (red) interacts with PSI subunits PsaH (magenta), PsaL (cyan), PsaA (orange) and PsaK (brown). Two LHCII α-chlorophylls (numbers 602 and 607, in blue) have energy transfer distances of 13 Å to 12 Å from two PSI chlorophylls (numbers 1151 and 1153, in green), respectively, that are coordinated by PsaA.

proteins[13] (Fig. 3a). A similar mode of association is observed between LHCI dimers, which allows all LHCI proteins to have their wider side turned to the reaction centre, enabling the maximum number of chlorophylls to face the core[24]. This arrangement results in relatively long distances between the membrane domains of adjacent monomers.

The half-moon shape of LHCI and the relatively loose and flexible coupling among its monomers may serve two important functions: (1) achieving the most efficient light harvesting and excitation energy migration, and (2) providing the basis for coping with ever-changing light intensities. Increased light intensities result in a sharp decrease in antenna size associated with the vulnerable PSII[30]; however, such an effect was not observed in LHCI. The composition—rather than the size—of this peripheral antenna varies with intensity[31]. It is possible that replacement of the Lhca2–Lhca3 heterodimer with an Lhca3–Lhca3 dimer results in longer trapping times, decreased efficiency in energy migration to the reaction centre, and dissipation of energy localized on Lhca3 by carotenoids.

The conservation of amino acid sequences between LHCII and the four LHCI monomers was found to be relatively poor. The four LHCI monomers share the LHCII general fold; that is, two long, tilted, intertwined transmembrane helices (A and B) and a shorter one roughly perpendicular to the membrane (C). The conservation of the fourth helix (D) was not apparent, and the fine structure of Lhca3 was found to be significantly different from the other three LHCI monomers (Fig. 3b). In Lhca3, helices A and B were much closer to each other, were almost parallel and were less intertwined. Consequently, Lhca3 bound its chlorophylls in a somewhat different position than the other three LHCI monomers. Recent reconstitution experiments clearly demonstrate that Lhca3 shares a similar fold to the others and binds its chlorophylls in the same fashion[32]. It therefore seems that when Lhca3 assembles by itself, it results in a similar structure to the others, but when it assembles in the context of the rest of PSI, it adopts a different conformation.

Subunit N

An electron density was identified at the luminal side of PSI close to Lhca2 and Lhca3. Because the volume of the density and the position at the lumen could be ascribed only to PsaN, we modelled into it the amino acids of this subunit (Fig. 3a). We used the available sequence from the plant *Phaseolus vulgaris* (accession number AA049652), which is expected to be almost identical to that from the related pea plants and differs from that of *A. thaliana* by only nine conservative substitutions. The electron densities in the region of PsaN are well defined, but at 3.4 Å resolution did not allow tracing of the amino acids sequentially. The positions of N and C termini were determined by secondary structural analysis, which suggested an approximately 30-amino-acid-long, predominantly α-helical stretch, at the N-terminal part of PsaN. In line with biochemical evidence[33,34], the structure of PsaN exhibits weak interactions with Lhca2 and Lhca3 (Fig. 3a).

Subunit N was first identified in a high ionic strength wash of PSI preparation from spinach chloroplasts[33,34]. The complete sequence of PsaN was first reported from barley[35] and has subsequently been reported in several other species of higher plants and green algae. An extensive crosslinking study revealed minimal interaction between PsaN and other small PSI subunits[36]. Putative crosslinking products between PsaN and PsaG and between PsaN and PsaF have been found, and specific inactivation of a nuclear gene encoding a PSI subunit N in *A. thaliana* plants has been reported[37]. The lack of PsaN

results in effects on plant growth and development under suboptimal conditions. Under standard growth conditions, plants compensate for deficient PSI by increasing the relative PSI content. It was proposed that PsaN is necessary for efficient interaction of PSI with plastocyanin. Our structure reveals no direct interaction with PsaG, PsaF or plastocyanin, but, as frequently occurred, indirect effects of the missing subunit might lead to the reported effects. Recent findings indicate that Lhca5 assembles onto Lhca2 (ref. 38); the position of PsaN (Fig. 4a) suggests it is involved in this process.

The PSI–LHCII supercomplex

The determined structure of plant photosystem I (PSI) provides the first relatively high-resolution structural model of a supercomplex containing a reaction centre and its peripheral antenna. This highly efficient nano-photoelectric machine is expected to interact with other proteins in a regulated and efficient manner. The most important interaction of PSI at the membrane level is with LHCII during state transition[8]. Plants adapt to changes in light quality by redistributing excitation energy between the two photosystems to enhance photosynthetic yield[39]. At high light intensities, LHCII migrates from PSII to PSI[40]. State transitions in higher plants are limited. In state II, additional light harvesting by PSI does not exceed 20% (ref. 41) and corresponds to an addition of up to a single LHCII trimer to PSI, forming a supercomplex of reaction-centre–LHCI–LHCII. Numerous experiments conducted in higher plants, including single particle analysis[42,43], support this model, but the detailed mechanism of state transitions remains unclear[44–46]. Even though LHCII is likely to interact with PSI at the PsaK side (which is less well resolved than the PsaG side), we superimposed LHCII on the current structure and found only one position with good fit (Fig. 4). In this model, only one of the three LHCII monomers was found to interact with the reaction centre, indicating that monomers may also fit well to the binding site. Recently it was reported that, in *C. reinhardtii*, CP29 associates with PsaH of PSI and was proposed to act as a docking site for LHCII during state transition[45]. Our model for the complex PSI–LHCII is compatible with the possibility that a similar interaction may take place in higher plants.

The complexity of PSI belies its efficiency: almost every photon absorbed by the PSI complex is used to drive electron transport. It is remarkable that PSI exhibits a quantum yield of nearly 1 (refs 47, 48), and every captured photon is eventually trapped and results in electron translocation. The structural information on the proteins, the cofactors and their interactions that is described in this work provides a step towards understanding how the unprecedented high quantum-yield of PSI in light capturing and electron transfer is achieved.

METHODS

PSI was isolated from pea and crystallized by a modified procedure that was described previously[12,13,49]. Changes to the procedure included additional sucrose gradient centrifugation in a SW60 rotor (Beckman) at 57,000 r.p.m. for 4 h, as well as substitution of citrate by succinate and adjustment of the pH to 6.0 for crystallization (see Supplementary Information). A crystal form was obtained by prolonged incubation with cryo solution containing a high concentration of PEG 6000. A similar procedure was used previously with crystals containing high water content (see Supplementary Information). The cryo solution contained 22 mM citrate, 22.5 mM MES/bis Tris (pH 6.7), 0.5% PEG 400, and 40% PEG6000. The crystals were washed in the same solution containing only 20% PEG 6000 and after 1 h were placed in the above solution for approximately 1 week. Before mounting, the crystals were incubated at room temperature for 1 day and frozen by liquid nitrogen or a nitrogen stream at 100 K. Detailed information on the X-ray data collection, evaluation and refinement at 3.4 Å resolution are provided in the Supplementary Information. As shown in Supplementary Fig. 1, the crystal lattice was changed from two PSI complexes in the asymmetric unit to a single complex maintaining the symmetry of P21.

Received 1 December 2006; accepted 19 February 2007.

1. Barber, J. Engine of life and big bang of evolution: a personal perspective. *Photosynth. Res.* **80,** 137–155 (2004).
2. Nelson, N. & Ben-Shem, A. The complex architecture of oxygenic photosynthesis. *Nature Rev. Mol. Cell Biol.* **5,** 971–982 (2004).
3. Nelson, N. & Ben-Shem, A. The structure of photosystem I and evolution of photosynthesis. *Bioessays* **27,** 914–922 (2005).
4. Jordan, P. *et al.* Three-dimensional structure of cyanobacterial photosystem I at 2.5 Å resolution. *Nature* **411,** 909–917 (2001).
5. Kurisu, G., Zhang, H., Smith, J. L. & Cramer, W. A. Structure of the cytochrome b_6f complex of oxygenic photosynthesis: tuning the cavity. *Science* **302,** 1009–1014 (2003).
6. Ferreira, K. N., Iverson, T. M., Maghlaoui, K., Barber, J. & Iwata, S. Architecture of the photosynthetic oxygen-evolving center. *Science* **303,** 1831–1838 (2004).
7. Loll, B., Kern, J., Saenger, W., Zouni, A. & Biesiadka, J. Towards complete cofactor arrangement in the 3.0 Å resolution structure of photosystem II. *Nature* **438,** 1040–1044 (2005).
8. Nelson, N. & Yocum, C. Structure and function of photosystems I and II. *Annu. Rev. Plant Biol.* **57,** 521–565 (2006).
9. Stroebel, D., Choquet, Y., Popot, J. L. & Picot, D. An atypical haem in the cytochrome b_6f complex. *Nature* **426,** 413–418 (2003).
10. Liu, Z. *et al.* Crystal structure of spinach major light-harvesting complex at 2.72 Å resolution. *Nature* **428,** 287–292 (2004).
11. Standfuss, J., Terwisscha van Scheltinga, A. C., Lamborghini, M. & Kuhlbrandt, W. Mechanisms of photoprotection and nonphotochemical quenching in pea light-harvesting complex at 2.5 Å resolution. *EMBO J.* **24,** 919–928 (2005).
12. Ben-Shem, A., Nelson, N. & Frolow, F. Crystallization and initial X-ray diffraction studies of higher plant photosystem I. *Acta Crystallogr. D* **59,** 1824–1827 (2003).
13. Ben-Shem, A., Frolow, F. & Nelson, N. The crystal structure of plant photosystem I. *Nature* **426,** 630–635 (2003).
14. Scheller, H. V., Jensen, P. E., Haldrup, A., Lunde, C. & Knoetzel, J. Role of subunits in eukaryotic Photosystem I. *Biochim. Biophys. Acta* **1507,** 41–60 (2001).
15. Jensen, P. E., Haldrup, A., Zhang, S. & Scheller, H. V. The PSI-O subunit of plant photosystem I is involved in balancing the excitation pressure between the two photosystems. *J. Biol. Chem.* **279,** 24212–24217 (2004).
16. Khrouchtchova, A. *et al.* A previously found thylakoid membrane protein of 14 kDa (TMP14) is a novel subunit of plant photosystem I and is designated PSI-P. *FEBS Lett.* **579,** 4808–4812 (2005).
17. Zygadlo, A., Robinson, C., Scheller, H. V., Mant, A. & Jensen, P. E. The properties of the positively charged loop region in PSI-G are essential for its "spontaneous" insertion into thylakoids and rapid assembly into the photosystem I complex. *J. Biol. Chem.* **281,** 10548–10554 (2006).
18. Ben-Shem, A., Frolow, F. & Nelson, N. Evolution of Photosystem I—from symmetry through pseudosymmetry to asymmetry. *FEBS Lett.* **564,** 274–280 (2004).
19. Lunde, C. P., Jensen, P. E., Haldrup, A., Knoetzel, J. & Scheller, H. V. The PSI-H subunit of photosystem I is essential for state transitions in plant photosynthesis. *Nature* **408,** 613–615 (2000).
20. Dashdorj, N., Xu, W., Cohen, R. O., Golbeck, J. H. & Savikhin, S. Asymmetric electron transfer in cyanobacterial Photosystem I: charge separation and secondary electron transfer dynamics of mutations near the primary electron acceptor A0. *Biophys. J.* **88,** 1238–1249 (2005).
21. Joliot, P. & Joliot, A. *In vivo* analysis of the electron transfer within photosystem I: are the two phylloquinones involved? *Biochemistry* **38,** 11130–11136 (1999).
22. Jolley, C., Ben-Shem, A., Nelson, N. & Fromme, P. Structure of plant photosystem I revealed by theoretical modeling. *J. Biol. Chem.* **280,** 33627–33636 (2005).
23. Morosinotto, T., Ballottari, M., Klimmek, F., Jansson, S. & Bassi, R. The association of the antenna system to photosystem I in higher plants. Cooperative interactions stabilize the supramolecular complex and enhance red-shifted spectral forms. *J. Biol. Chem.* **280,** 31050–31058 (2005).
24. Ben-Shem, A., Frolow, F. & Nelson, N. Light-harvesting features revealed by the structure of plant photosystem I. *Photosynth. Res* **81,** 239–250 (2004).
25. Ganeteg, U., Strand, A., Gustafsson, P. & Jansson, S. The properties of the chlorophyll a/b-binding proteins Lhca2 and Lhca3 studied *in vivo* using antisense inhibition. *Plant Physiol.* **127,** 150–158 (2001).
26. Schmid, V. H., Paulsen, H. & Rupprecht, J. Identification of N- and C-terminal amino acids of Lhca1 and Lhca4 required for formation of the heterodimeric peripheral photosystem I antenna LHCI-730. *Biochemistry* **41,** 9126–9131 (2002).
27. Ihalainen, J. A. *et al.* Pigment organization and energy transfer dynamics in isolated photosystem I (PSI) complexes from *Arabidopsis thaliana* depleted of the PSI-G, PSI-K, PSI-L, or PSI-N subunit. *Biophys. J.* **83,** 2190–2201 (2002).
28. Durnford, D. G. *et al.* A phylogenetic assessment of the eukaryotic light-harvesting antenna proteins, with implications for plastid evolution. *J. Mol. Evol.* **48,** 59–68 (1999).
29. Morosinotto, T., Castelletti, S., Breton, J., Bassi, R. & Croce, R. Mutation analysis of Lhca1 antenna complex. Low energy absorption forms originate from pigment–pigment interactions. *J. Biol. Chem.* **277,** 36253–36261 (2002).
30. Anderson, J. M., Chow, W. S. & Park, Y.-I. The grand design of photosynthesis: acclimation of the photosynthetic apparatus to environmental cues. *Photosynth. Res* **46,** 129–139 (1995).
31. Bailey, S., Walters, R. G., Jansson, S. & Horton, P. Acclimation of *Arabidopsis thaliana* to the light environment: the existence of separate low light and high light responses. *Planta* **213,** 794–801 (2001).
32. Mozzo, M., Morosinotto, T., Bassi, R. & Croce, R. Probing the structure of Lhca3 by mutation analysis. *Biochim. Biophys. Acta.* **1757,** 1607–1613 (2006).

33. Ikeuchi, M. & Inoue, Y. Two new components of 9 and 14 kDa from spinach photosystem I complex. *FEBS Lett.* **280,** 332–334 (1991).
34. He, W. Z. & Malkin, R. Specific release of a 9-kDa extrinsic polypeptide of photosystem I from spinach chloroplasts by salt washing. *FEBS Lett.* **308,** 298–300 (1992).
35. Knoetzel, J. & Simpson, D. J. The primary structure of a cDNA for PsaN, encoding an extrinsic lumenal polypeptide of barley photosystem I. *Plant Mol. Biol.* **22,** 337–345 (1993).
36. Jansson, S., Andersen, B. & Scheller, H. V. Nearest-neighbor analysis of higher-plant photosystem I holocomplex. *Plant Physiol.* **112,** 409–420 (1996).
37. Haldrup, A., Naver, H. & Scheller, H. V. The interaction between plastocyanin and photosystem I is inefficient in transgenic *Arabidopsis* plants lacking the PSI-N subunit of photosystem I. *Plant J.* **17,** 689–698 (1999).
38. Lucinski, R., Schmid, V.H., Jansson, S. & Klimmek, F. Lhca5 interaction with plant photosystem I. *FEBS Lett.* **580**, 6485–6488 (2006); published online 7 November 2006.
39. Bellafiore, S., Barneche, F., Peltier, G. & Rochaix, J. D. State transitions and light adaptation require chloroplast thylakoid protein kinase STN7. *Nature* **433,** 892–895 (2005).
40. Kyle, D. J., Staehelin, L. A. & Arntzen, C. J. Lateral mobility of the light-harvesting complex in chloroplast membranes controls excitation energy distribution in higher plants. *Arch. Biochem. Biophys.* **222,** 527–541 (1983).
41. Allen, J. F. Cyclic, pseudocyclic and noncyclic photophosphorylation: new links in the chain. *Trends Plant Sci.* **8,** 15–19 (2003).
42. Consoli, E., Croce, R., Dunlap, D. D. & Finzi, L. Diffusion of light-harvesting complex II in the thylakoid membranes. *EMBO Rep.* **6,** 782–786 (2005).
43. Kouril, R. *et al.* Structural characterization of a complex of photosystem I and light-harvesting complex II of *Arabidopsis thaliana*. *Biochemistry* **44,** 10935–10940 (2005).
44. Haldrup, A., Jensen, P. E., Lunde, C. & Scheller, H. V. Balance of power: a view of the mechanism of photosynthetic state transitions. *Trends Plant Sci.* **6,** 301–305 (2001).
45. Kargul, J. *et al.* Light-harvesting complex II protein CP29 binds to photosystem I of *Chlamydomonas reinhardtii* under State 2 conditions. *FEBS J.* **272,** 4797–4806 (2005).
46. Takahashi, H., Iwai, M., Takahashi, Y. & Minagawa, J. Identification of the mobile light-harvesting complex II polypeptides for state transitions in *Chlamydomonas reinhardtii*. *Proc. Natl Acad. Sci. USA* **103,** 477–482 (2006).
47. Trissl, H.-W. & Wilhelm, C. Why do thylakoid membranes from higher plants form grana stacks? *Trends Biochem. Sci.* **18,** 415–419 (1993).
48. Sener, M. K. *et al.* Evolution of the excitation transfer network in photosystem I from cyanobacteria to plants. *Biophys. J.* **89,** 1630–1642 (2005).
49. Amunts, A., Ben-Shem, A. & Nelson, N. Solving the structure of plant photosystem I—biochemistry is vital. *Photochem. Photobiol. Sci.* **4,** 1011–1015 (2005).

Supplementary Information is linked to the online version of the paper at www.nature.com/nature.

Acknowledgements We thank the ESRF for synchrotron beam time, and staff scientists of the ID 14, ID 29 and ID 23 station clusters for their assistance. We also thank F. Frolow and J. Hirsh for valuable guidance and advice in crystallography. This work was supported by The Israel Science Foundation.

Author Information Atomic coordinates and structure factor files were deposited in the Protein Data Bank under accession number 2O01. Reprints and permissions information is available at www.nature.com/reprints. The authors declare no competing financial interests. Correspondence and requests for materials should be addressed to N.N. (nelson@post.tau.ac.il).